Malaysian Journal of Civil Engineering 30(1):37-56 (2018)

STRUCTURAL PERFORMANCE OF SPACE TRUSSES UNDER FIRE

Amr M. Ibrahim, Ahmed A. Elshafey, Boshra A. El-taly* & Kamel S. Kandil

Civil Engineering Department, Faculty of Engineering, Minoufia University, Gamal Abdul-Nasser Street, Minoufia, Egypt

*Corresponding Author: *Boushra_Eltaly@yahoo.com*

Abstract: An experimental program was designed in the current work to capture the structural behavior of two different space trusses under static loads and under increasing the temperature at the truss nodes up to failure. The results of the two space trusses tested include the central deflection of the truss and the axial forces in truss members under the applied loads and temperature. Also analytical studies based on finite element method for the two tested trusses are introduced in this paper. A comparison between experimental work and analytical study is presented and discussed. The finite element simulation gives good agreement with the experimental results. Also the results of the current work indicate that increasing the temperature causes a local failure due to fusion of the node at which the temperature was applied.

Keywords: *Space trusses, test setup, fire conditions, finite element simulation.*

Article history:
Received 23 January 2017
Received in revised form 25 April 2017
Accepted 20 July2017
Published online 30 April 2018

1.0 Introduction

Space trusses are three dimensional structures assembled of linear elements. These elements are arranged in a way that ensures a three dimensional force transfer from the load application point to supports. Space structures have the ability of covering large areas. They attracted architects attention because they gave freedom in design and a pleasing appearance (Iffland 1982, Iffland 1987, Lan 1985 and Lan 1999). Space truss connection has an important effect on the behavior and the cost of these structures. The MERO space truss joint system is a multidirectional system. This type of connection allows up to eighteen tubular members to be connected together through a spherical node at various angels. Another system called triodetic in which, bars are folded and cut to precise angles at their ends and inserted in special slots made in the nodes using pressure. One of the most common connections used for steel space trusses is the connections obtained by joining the end-flattened tubes with a single bolt. The advantages of such connections are reduced costs and fast assemblage of the truss, and their disadvantages are the eccentricities and stiffness reduction of the truss members

All rights reserved. No part of contents of this paper may be reproduced or transmitted in any form or by any means without the written permission of Penerbit Universiti Teknologi Malaysia

(Schmidt *et al*. 1982, Hanaor *et al*. 1989, EL-Sheikh 1996, De Andrade *et al*. 2005, El-Shami *et al*. 2016 and Feng *et al*. 2016).

Space structures might face a brittle type of failure. This failure may be initiated by the overloading and consequent buckling of compression members (Mezzina *et al*. 1975, Schmidt *et al*. 1976, Collins 1981, Smith 1988, El-Bakry 1995, Bakr *et al*. 2016 and Bakr 2014). Several studies have been done to improve the nonlinear behavior of space truss. Schmidt and Hanaor (1979) introduced an artificial ductility to the compression member by building into it a Force Limiting Device (FLD). FLD is a device used to provide the strut (compression member) with an elastic-plastic load-deflection characteristic. El-Sheikh (1991) increased the ductility of the space truss using over-strengthened top chord members. El-Sheikh (1991), El- Sheikh and El-Bakry (1996) and Shaaban (1997) performed a series of experimental tests and numerical analyses to improve the overall behavior of the space trusses using the composite action between the upper concrete slab and the top members of the truss. Eltaly (2010) investigated the behavior of space trusses with top ferrocement slabs. Her results showed that the ferrocement slab decreases the force in the top chord members. Nawer (2014) improved the nonlinear behavior of space trusses using top sandwich panel. The top sandwich panel slab is considered one of the common types of slabs which are used to cover the steel structure for thermal insulation and light weight.

The incremental reduction in the strength of steel with increasing temperature is a well-known phenomenon which, in the event of fire, can lead to a catastrophic collapse of structures. Bujakas (1998) reported on the shape control of space structures, and stated that manufacturing, assemblage, and deployment errors, as well as thermal deflections, are recognized as major causes of shape distortion in large space designs. Chilton (2000) showed that with the thermal movements associated with the normal changes in ambient temperature, it is desirable to provide appropriate sliding bearings to absorb expansions; otherwise, the expansion may induce high compressive forces in the space grid due to the rigid restraint. Yarza *et al*. (1993) processed a mathematical model to find the consequent reduction in strength of the steel bars over a given time. The researcher stated that corner-supported space grids are most vulnerable in fire, due to the potential catastrophic failure of the diagonal web members immediately adjacent to the supports or to bending failure due to the collapse of the chord members. Alinia and Kashzadeh (2006) studied the influence of the flexibility of substructures on the behavior of space truss domes, by predicting the thermal forces and stresses transmitted to the columns. They introduced a uniform thermal loading to six studied double layer space truss models. For each model, fifteen different support conditions plus the two extreme pinned and roller supports were studied. Alinia and Kashzadeh (2006) then completed their studies by studying the effect of support flexibility on the behavior of the double layer space truss domes structures subjected to gradient and partial loadings.

From previous discussions, it can be concluded that the structural performances of space trusses under static and dynamic loads up to failure were estimated by various previously published researches and on the other hand their behavior under fire needs to be estimated. The current work presented construction and testing of two space trusses (Truss#1 and Truss#2) to study the effect of fire on their structural performance up to failure. Total five tests were carried out on the two trusses; three tests for truss#1 and two tests for truss#2. The space trusses tested were simulated by a finite element program, ANSYS software. The comparison between the results of the experimental and finite element models of these types of space trusses is presented.

2.0 Experimental Work

2.1 Specimens Details

In the current work, two different corner supported double layer space trusses were constructed and tested under static loads and under fires up to failure. The two trusses have the same view as shown in Figure 1 and they are different in the overall dimensions (L, B and h), the members dimension and the type of connections. The first space truss (truss#1) has 3000 mm length (L), 3000 mm width (B) and 500 mm depth (h). All the members of truss#1 were tubular cross-section with 42.4 mm outer diameter and with 3.25 mm thickness. The members were connected together with MERO connections. The second tested truss (truss#2) has overall dimensions of 2850 x 2850 x 500 mm. All of the truss members of truss#2 were made of tubular cross-sections with 25 mm outer diameter and with 1.25 mm wall thickness. The four corner diagonal members of truss#2 were chosen to be a tubular cross-section with 32 mm outer diameter and with 1.5 mm wall thickness. All the members of truss#2 were connected together using the end-flattened connection.

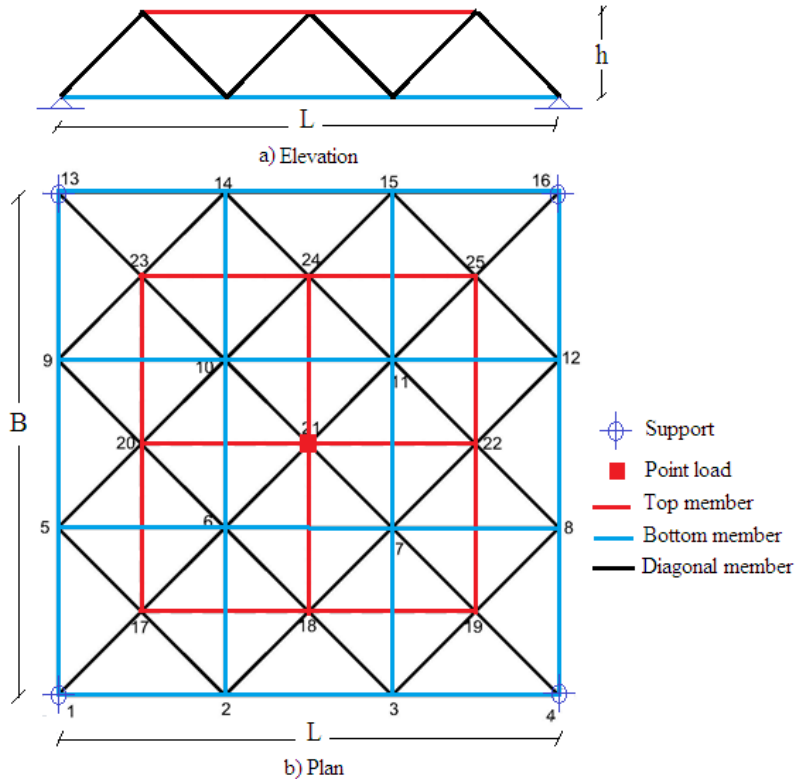

Figure 1: Tested trusses layout

2.2 Assembling Process of The Space Trusses

The supporting frame of the tested trusses consists of four columns with SIB200 and with 800 mm length. These columns are supported on four reinforced concrete (RC) footings with 400 x 400 x 400 mm overall dimensions and each footing was reinforced by 5Φ8 mm in the two directions as shown in Figure 2. The four footings were connected together by SIB120 steel beams in all directions. Also the columns were connected together in all directions by SIB120 beams as shown in Figure 3 to prevent the side sway. The assembling process of the space truss#1 members was carried out through four steps. The first step was the classification process of the truss members to upper, lower and diagonal members and the MERO connections to connections with 3, 4, 5, 6 and 8 holes. The second step was the determination of the location of the lower MERO connections by drawing a layout of these connections on the supporting frame then the lower connections were inserted in their locations. At the third step, the lower chord members were connected to each other through these connections. The fourth step was determining the location of the MERO connections of the upper chord members then the diagonal members were connected to these connections after that the

top members were joined to these connections as shown in Figure 4. Finally, all the connections were well tightened to increase the truss stiffness and to make the truss acts as one unit. The truss was supported on the supporting frame through four connections. Each connection consisted of pipe with 200 mm height. Two plates with 200 x 200 mm dimensions and 10 mm thickness were welded on the two ends of the pipe. Then the top plate was welded to the corner truss connection and the bottom plate was connected with the supporting frame column through four bolts as shown in Figure 5.

Truss#2 connections were made by flattening the ends of the member and assembling them with one bolt (M17 bolt) as shown in Figure 6. The lower truss members were assembled first, followed by the upper chord members. Then the diagonal members were connected to the upper and lower chord members. Finally the truss placed on the supporting frame see Figure 7.

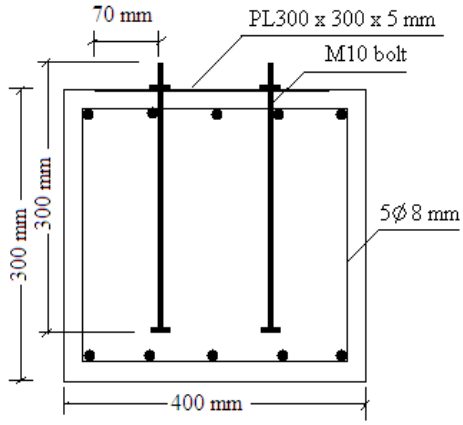

Figure 2: Footing details

Figure 3: Supporting frame

Figure 4: Assembling process of truss#1 members

Figure 5: Connection between truss#1 and supporting frame

Figure 6: Truss#2 connection

Figure 7: Assembling process of the truss#2 members

2.3 Testing of İndividual Truss Members

Three specimens of each member of the two trusses were tested under compression force to obtain the buckling and post-buckling behavior of the truss members. The members were prepared by welding two stiff circular plates with 100 mm diameter and 30 mm thickness at the two ends. Each member was inserted in the supporting frame as shown in Figure 8. Tensile tests were conducted to determine the stress–strain curve of the truss members. Two specimens; were taken from tubes with 1000 and 866 mm length. The specimens were prepared by adding steel bar with 220 mm length at the two ends of the members. These steel bars were added to avoid flattening of the members ends under the gripping force. The test was carried out on the universal testing machine. The samples were placed in the machine and gripped by the machine ends as shown in Figure 9. Then the test was started by pulling the two ends of the member till its failure.

For truss#1, the upper and lower chord member with 1000 mm length started to buckle at 110 kN axial load, while the diagonal member with 866 mm length started to buckle when the load reached to 250 kN and the member failure is presented in Figure 9. The relation between the load and the axial shortening is represented in Figure 10. The relation between the load and the axial shortening for truss#2 members are represented in Figure 11 and Figure 12. From the two figures, it can be shown that the chord member buckled at 27.08 kN axial load, the diagonal member buckled when the load reached to 23.05 kN load on the other hand the corner member buckled at an axial load of 199.94 kN. The relation between stress and strain curve obtained from the tension test is indicated in Figure 13. From this curve, the modulus of elasticity, yield stress and ultimate strength of the truss were considered as 215 GPa, 380 MPa and 525 MPa, respectively.

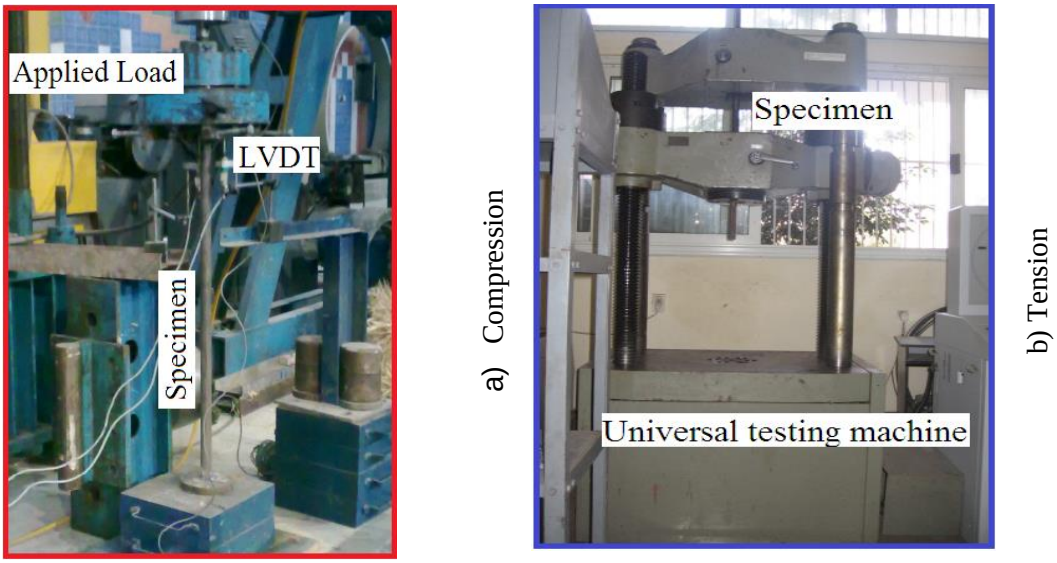

Figure 8: Truss member Tests

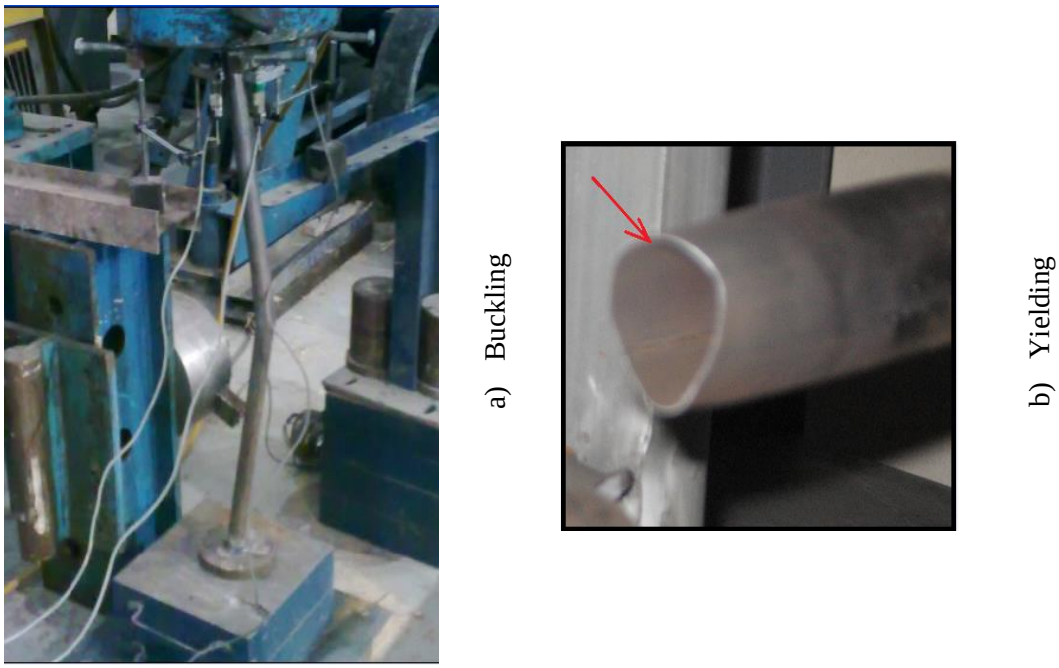

Figure 9: Member failure

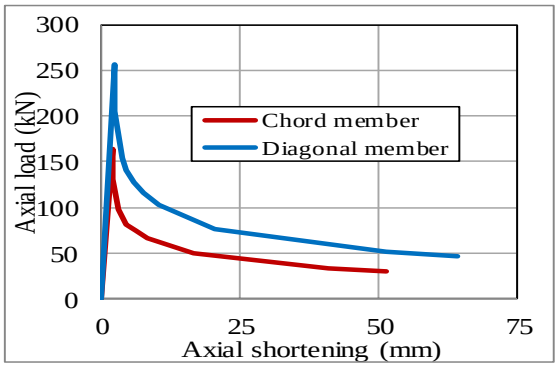

Figure 10: Load-axial shortening curve for chord and diagonal member of truss#1

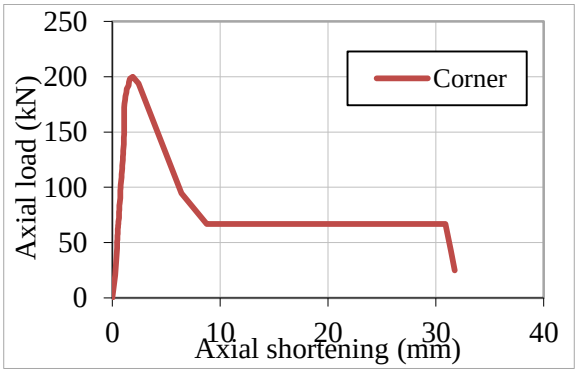

Figure 11: Load-axial shortening curve for corner member of truss#2

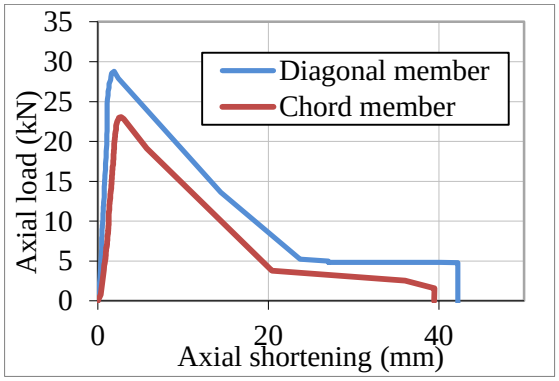

Figure 12: Load-axial shortening curve for chord and diagonal member of truss#2

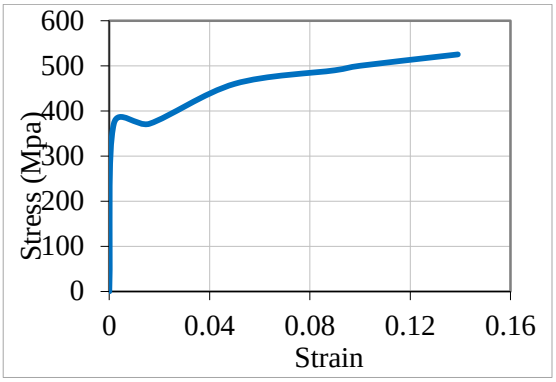

Figure 13: Stress-strain curve

2.4 Truss Testing Process

A hydraulic jack with 500 kN capacity and the displacement dial gauges with an accuracy of 0.01 mm were installed on the space truss as shown in Figure. 14. Also the strain was measured at selected members (see Figure. 15) by means of an extensometer. The testing process of truss#1 was performed in three stages. In the first stage, a concentrated load was applied at top mid joint of the truss (joint#21) with 5 kN load increment. In the second stage, 80 kN a constant static load was applied at the top mid joint and an increase in temperature (from 100 °C to 400 °C) was applied at two lower joints of the truss joints (7 and 11). In the third stage, 80 kN a constant static load was applied at the top mid joint and a uniform increasing in temperature was applied at four lower joints of the truss joints (6, 7, 10 and 11).

The testing process of truss#2 was performed in two stages. A concentrated load was applied at the top mid joint of the truss#2 (joint#21) with 5 kN load increment in the first stage. In the second phase, the four lower joints (6, 7, 10 and 11) were subjected to fire load and the truss was loaded by 20 kN constant static load applied at joint#21. In this test, the temperature increased from 300 °C to 900 °C with a 200 °C temperature increment. The time increment of temperature is 30 minutes.

a) Without fire b) With fire

Figure 14: Test setup

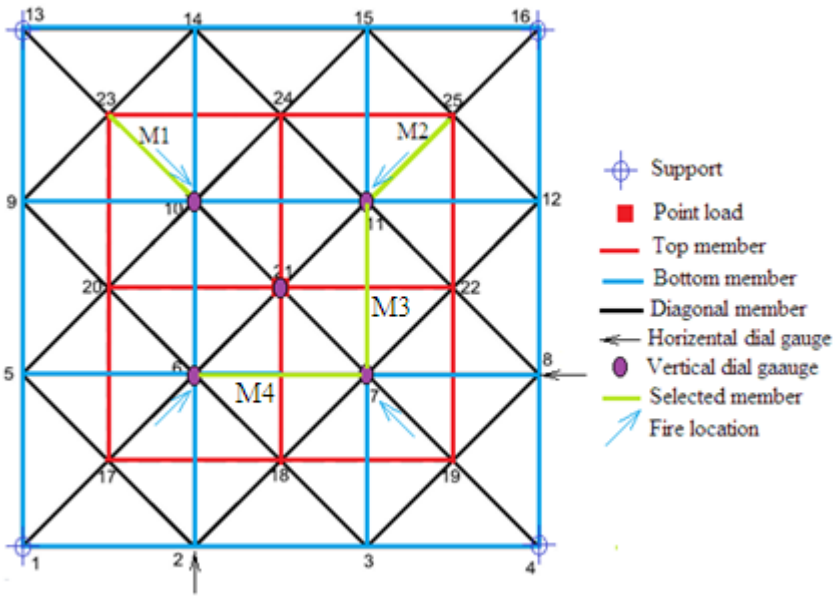

Figure 15: The location of displacement gauges, strain gauge and fire applied

3.0 Finite Element Simulation

The two trusses tested were simulated using the finite element program (ANSYS Version 12). The members of truss#1 were represented in the FEM program as Link8 elements. Each element has three degrees of freedom at each node; translations in x, y and z directions. This element is defined by two nodes, the cross-sectional area and its material properties. The truss was analyzed under the same conditions taken in the experimental test. The material properties were represented as the experimental results and the truss supports were considered as hinged supports. The truss was analyzed in three stages. In the first stage, the truss was analyzed through series of linear static analyses with different static concentrated load at joint#21; 5 kN, 10 kN up to 80 kN applied load. In each series of linear analysis, the displacements and the forces in the members were recorded and used in the comparisons with the experimental results. The second stage was held by applying a fire load (increase in temperature) to the lower joint#7 and #11 and applying a load of 80 kN concentrated at joint#21. In the third stage, the truss was subjected to a uniform increase in temperature at lower joints (6, 7, 10 and 11) in addition to the static load with value 80 kN applied to the joint#21.

For truss#2, each member was simulated by two Link8 elements and COMBIN39 element as shown in Figure 16 (Eltaly 2010). Link8 element has three degrees of freedom at each node; translations in x, y and z directions. COMBIN39 element has longitudinal or torsional capability in several dimensional applications. The element with longitudinal capability is a tension-compression element with three DOFs at each node (translations in the nodal x, y, and z directions). The element with torsional capability is a purely rotational element with three DOFs at each node; rotation about the nodal x, y, and z axes. Link8 element was adjusted to be very stiff such that it has no effect on the behavior of the truss model. The nonlinear material behavior was developed by COMBIN39 element with longitudinal capability. In order to make the model stable, Combine39 element with torsional capability is built on the COMBIN39 element with longitudinal capability. The additional COMBIN39 element should be defined with large stiffness to ensure the stability of the space truss element. COMBIN39 element was defined by two nodes and a nonlinear generalized force-deflection curve. This curve represents the nonlinear behavior of the truss member in the tension and compression. The force-deflection curve should be inserted such that deflections are increased from the compression to the tension. The last input deflection must be positive. Segments tending towards vertical should be avoided. The displacement control technique was used to obtain the behavior of the member up to failure. This technique was used because the strength of space trusses regularly degrades after reaching the plastic stage of the behavior. The truss supports were considered as hinged supports. In the case of the fire, the truss was subjected to a uniform increase in temperature at selected lower joints. The finite element simulation was presented in Figure 17.

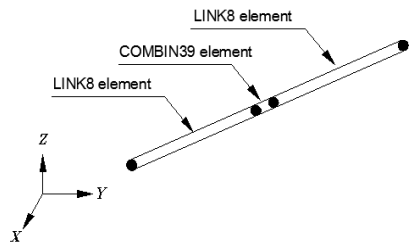

Figure 16: Modelling space truss members

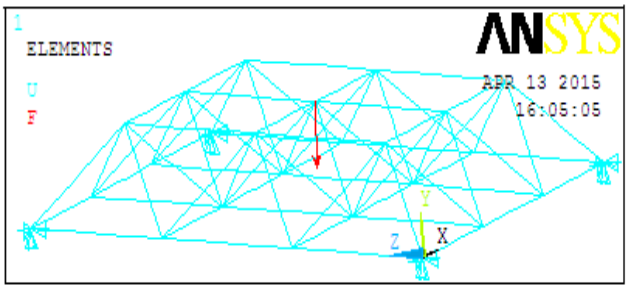

Figure 17: Finite element simulation

4.0 Results And Discussion

4.1 Truss#1

The results obtained from the finite element simulation for truss#1 were represented as relations between load-displacement, load-axial force, temperature-displacement and temperature-axial force for the selected joints and members (see Figure 15) were compared with the experimental results in the current section. For the first test, the relationship between the applied load and the corresponding mid-span deflection (at point#21) is shown in Figure 18. From this figure, it can be shown that the numerical load-central vertical deflection relationship is linear up to a load of 90 kN with central deflection 3.145 mm. At this load, local failure at a corner joint (at the welding between the tubular member and the cone of the member's end) occurred as shown in Figure 19. The collapse of this connection leads to failure of all the surrounding members and it leads to a large deflection to all surrounding joints. Also from these figures, it can be observed that the failure occurred in the weak point of the member. The strain of tested truss members as the load is applied was measured by means of an extensometer. Knowing the strains, it will be easy to calculate the stresses and the forces in the members for comparison purpose with the numerical model. The relation between load and axial force is presented in Figure 20. This relation is linear till the failure occurred at the location of the applied load. From Figure 18 and Figure 20, the margin of error between the results of FE simulation and experimental work is about 11%, which is considered acceptable.

Figures 21 to 27 present the results of the tested truss#1 for the second stage of the test as obtained from the experimental program and numerical model. From Figure 21, it can be clearly seen that the displacement was recorded 23.2 mm at temperature 200°C for point#7 from the FE simulation while the displacement of this point at the same temperature was measured as 20.88 mm from the experimental work. At temperature 300°C, the displacement at point#7 is 33.55 mm and 30.19 mm from FE simulation and experimental work; respectively, and at temperature 400°C, the displacement for

point#7 is 43.9 mm and 39.5 mm from FE simulation and experimental work; respectively. From Figure 22 and Figure 23, it can be concluded that the difference between the axial forces in the selected members as obtained from the experimental and FE simulation for the second test stage does not exceed 10%. Figures 24 and 25 showed local failures occurred in the truss joints at the joints subjected to the increase in temperature (at point#7 and 11) from the experimental test and numerical model. Figure 26 shows the variety in deflection at joint#6 and joint#7 as a result of their location from the fire source. The deflection in joint#6 decreases by 77% than that measured for joint#7. Also the axial force in the two selected members (M1&M2) was calculated as presented in Figure 27. From Figure 27, it can be observed that the members near the fire source (M2) are subjected to a high stress than that one far away from the heat source (M1). Also from the results indicated in the two figures (Figures 26 and 27), it can be concluded that the temperature transfers slowly in the truss members when half the truss was subjected to fire.

For the third test stage, the failure in this case occurred at 400 °C temperature as a result of local failure in the truss joints as shown in Figures 28 and 29. The experimental test indicates that the deflection at all recorded joints (6, 7, 10&11) are the same and the axial forces in the two members (M1&M2) are equal. The relation between the displacement and temperature for the third test as obtained from the experimental and numerical results is illustrated in Figure 30. From this figure, it can be observed that the experimental and numerical curves are very close and the difference between their results do not exceed 15%. Figure 31 illustrated that by increasing the temperature to 200°C, the axial force becomes 99.69 kN and 110.77 kN from the experimental and numerical results; respectively, and by increasing the temperature to 300°C, the axial force becomes 153.081 kN and 170.09 kN from the experimental and numerical results; respectively. Additionally, when the temperature was increased to 400°C the axial force in the selected member#1 is 229.4 kN and 206.46 kN as obtained from the numerical and experimental results; respectively. This shows that the structure is more vulnerable at higher temperature as the axial force and deflection increase by about 2000% and by 1500% respectively by applying 400^{o} C.

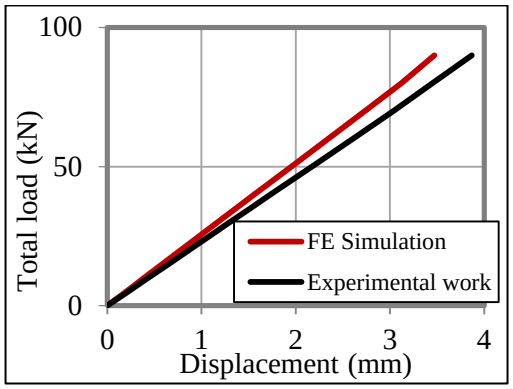

Figure 18: Load-deflection curves for the first test of truss#1 at joint#21

Figure 19: Collapse in the corner member from the first test of truss#1

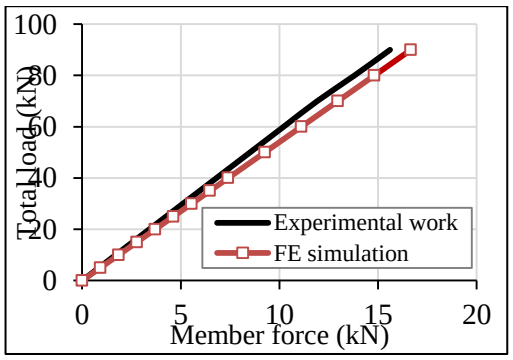

Figure 20: Axial force for M1&M2 from the first test of truss#1

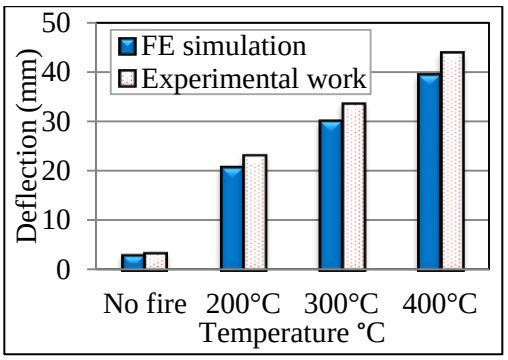

Figure 21: Temperature- deflection curve at joint#7 for the second test of truss#1

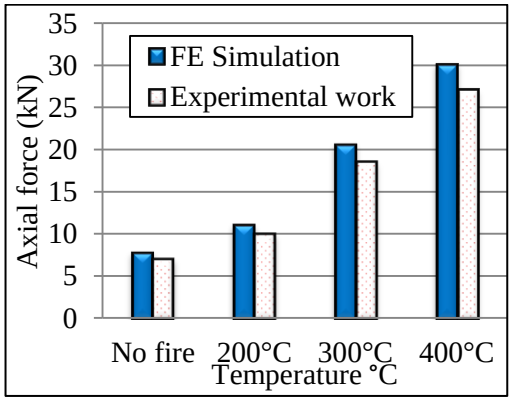

Figure 22: Axial force for M1 from the second test of truss#1

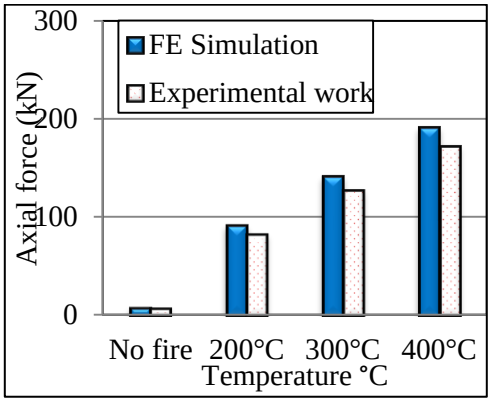

Figure 23: Axial force for M2 from the second of test of truss#1

Figure 24: Collapse in connections (7&11) from the second test of truss#1

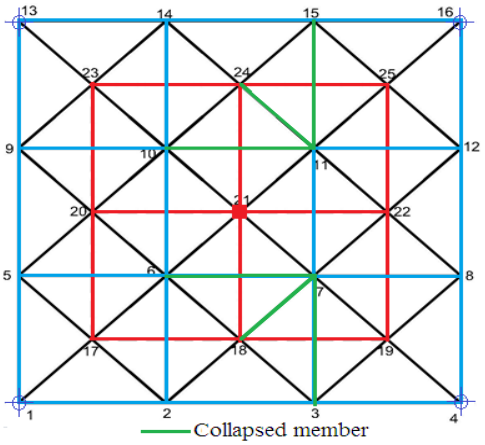

Figure 25: Collapsed members from the second test of truss#1

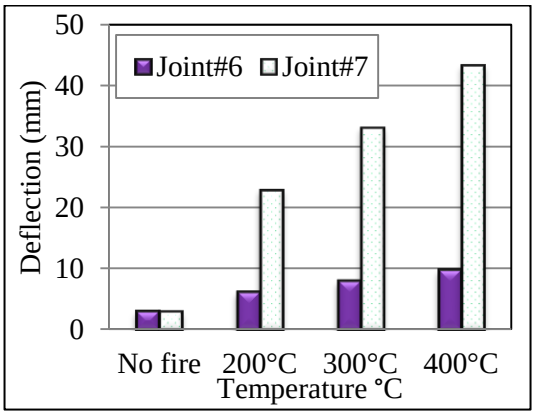

Figure 26: Experimental temperature-deflection curve for joint#6&7 from the second test of truss#1

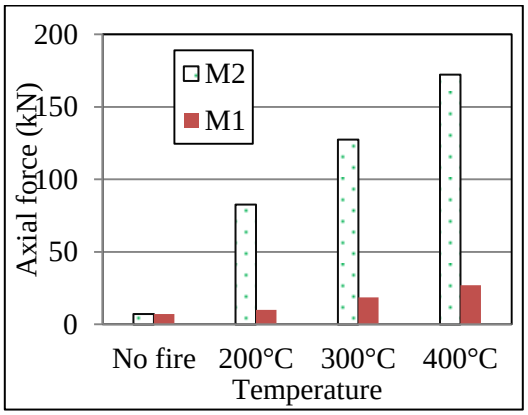

Figure 27: Experimental temperature-axial force curve for M1&M2 from the second test of truss#1

Figure 28: Collapse in connections (20&23) from the third test of truss#1

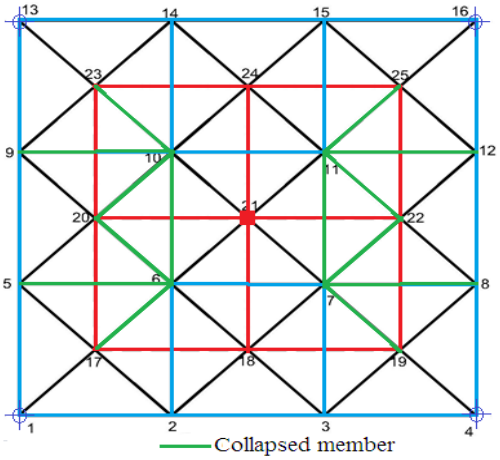

Figure 29: Numerical collapsed members from the third test of truss#1

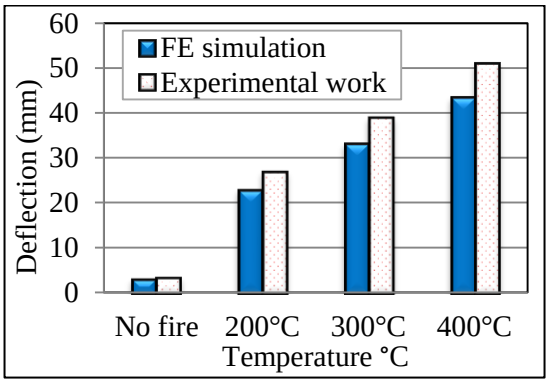

Figure 30: Temperature- deflection curves at joints#6 &7 from the third test of truss#1

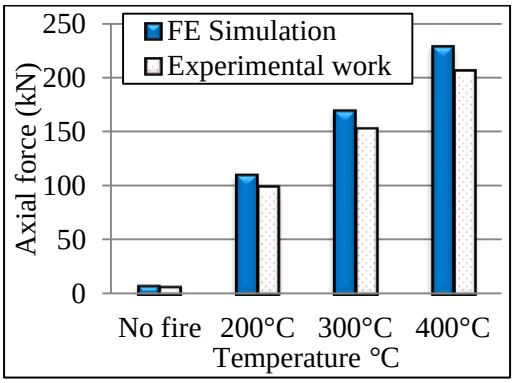

Figure 31: Axial force for M1&M2 from the third test of truss#1

4.2 *Truss#2*

In this section, the experimental results of the tested truss#2 without fire are presented and discussed. Figure 32 presents the load-deflection curves at joint#10. This figure indicated that the relation between load and corresponding deflection are linear till 70 kN total load and 22.43 mm as obtain from the experimental work. At this load, the failure occurred in the truss due to buckling of a top member that attached directly to the joint at which the load was applied (see Figure 33). After that, the truss was not able to carry a more applied load so that the applied load decreases to be 48 kN. Also from Figure 32, it can be seen a good agreement between the results obtained from the experimental and numerical analysis especially in the linear zone. The ANSYS results showed that space truss#2 collapsed at 68.20 kN total load and 25 mm corresponding

deflection at joint#10 due to buckling of showing members in Figure 34. Then the applied load is decreased with large increasing in the deflection till 50.08 kN applied load and 40.04 mm corresponding deflection. Figure 35 shows the axial forces in members M3 and M4 (see Figure 15) as obtained from the experimental and the numerical analysis. The axial force at the end of the linear zone is to be 21.2 kN from the numerical analysis and is 21.82 kN from the experimental test. From the previous results, it is clear that the difference between two results does not exceed 5%.

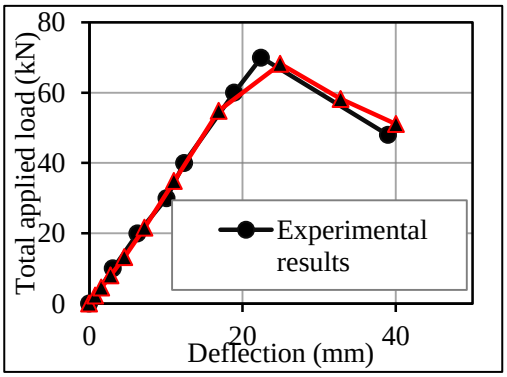

Figure 32: Load-deflection curves from the first test of truss#2

Figure 33: Experimental collapsed members from the first test of truss#2

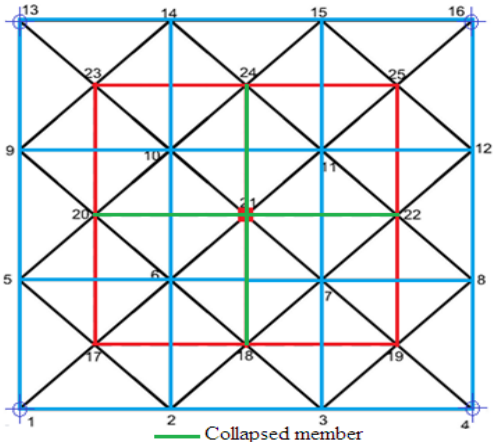

Figure 34: Numerical collapsed members from the first test of truss#2

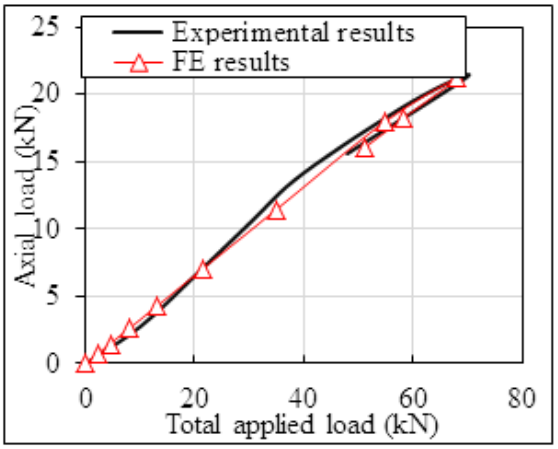

Figure 35: Axial force for M3 and M4 form the first test of truss#2

The results of the studied space truss#2 under the effect of fire are presented in Figures 36 to 38. Figure 36 shows a comparison between the increase in temperatures (from 300°C to 900°C) and the deflection at joint#10 as obtained from the experimental work and numerical model. Figure 37 shows a comparison between the experimental work and numerical model results in term of axial forces in M3 member with different temperatures. From the two figures, it can be concluded that the difference between the experimental and the numerical results do not exceed 10%. From Figure 36, one can observe that the truss deflections increase with increasing the applied temperature. On the other hand, Figure 37 shows that the axial forces in bottom member (M#3) increase by applying 300 °C temperature then the forces decrease by increasing the applied temperature. That is because the collapse in the truss started in appearing at applying 300 °C temperature as a local failure at the four joints at the source of the temperature as illustrated in Figure 38. This failure causes decrease in the truss stiffness with the temperature increase. From these results, it can be concluded that the heat transfer from the joints to the members was very slow that causes buckling or yielding in the truss members.

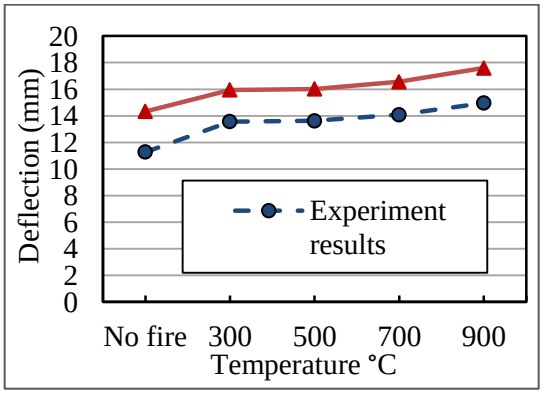

Figure 36: Temperature-deflection curve for joint#10 from the fire test of truss#2

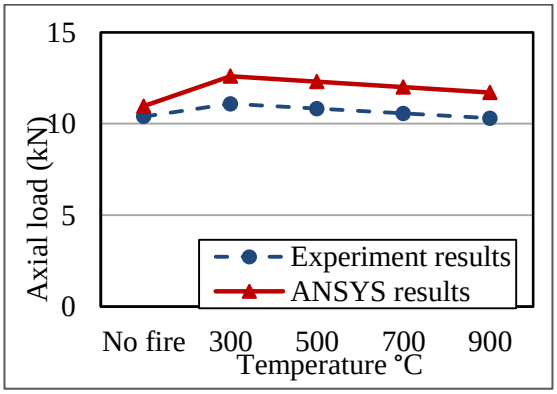

Figure 37: Axial force for M3 form the fire test of truss#2

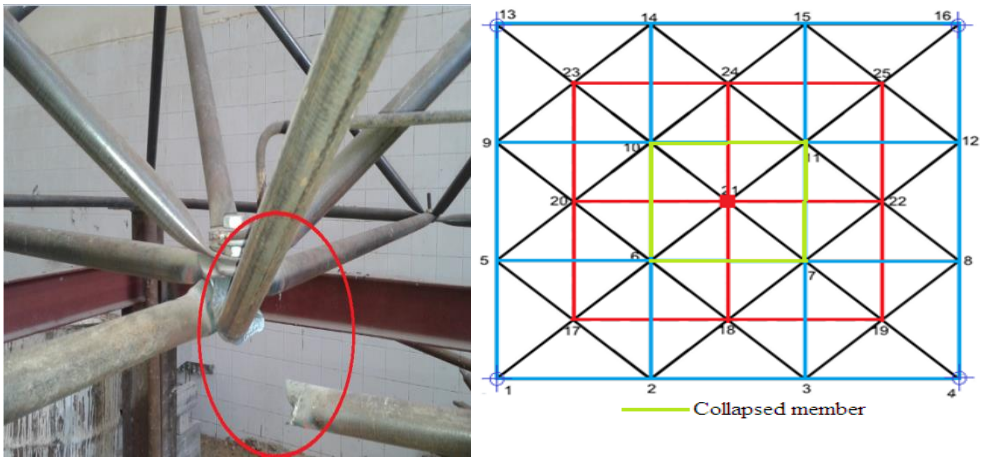

Figure 38: Collapsed members form the second test of truss#2

5.0 Conclusion

The current research presented tests on two space truss to estimate the structural behavior of these structures under the effect of fire. Truss#1 was tested in three testing stages and the truss#2 was tested in two testing stages. In the first testing stages, a concentrated load was applied at the middle of the truss. The second testing stage took place by applying a constant static load in addition to increase in temperature to two lower joints of the truss. The third stage test is similar to the second test except that a uniform increase in temperature was also applied to the four lower joints of the truss. In general, good agreement can be clearly seen between the results obtained from the finite element program and the experimental test. From the results of the current experimental work and analytical model, it can be noted that:-

For the space truss#1

- From the experimental results of the space truss without fire, it is found that the truss collapsed locally in corner joints due to the high stiffness of the tested truss at 90 kN total applied load.
- From the two experimental tests of the fire, it is observed that the failure occurred is due to the loss of tension members that are directly attached to the heated joints, due to the increase in tension force (these members are separated from the connection at the weld location due to the fusion of this zone).
- In the second model test in which half the truss was heated, the deflection of the heated joints increased than that joints which are far away from the heat source, this increase in deflection reached about 77%. It shows a significant increase due to the fire load.

- From the results of the second test, it can be seen that the axial force induced in the members attached directly to the heat source was so big in value (172.7 kN) than that induced in the members that are far away from the heat source which found to be nearly 30 kN (this shows the great effect of the fire on the truss).
- From the results obtained from the third test model, it is found that the deflection of the heated joints, increased by a percentage that is nearly equal to 20% than that deflection obtained from the second model test at the same heated joints and by a percentage that equals nearly 75% than that deflection obtained from the first model test.
- Also from the results of the third test, it can be concluded that subjecting the four lower joints of the truss to the increasing temperature led to increasing of the axial force induced in the members that are attached directly to the heated joints from (172.7 kN) that obtained from the second test to (206.46 kN) at 400 ^{o}C temperature.

For the space truss#2

- The failure occurred in the truss#2 due to buckling of a top member that is attached directly to the joint at which the load was applied.
- After the occurrence of the buckling in member, brittle failure occurs in the truss.
- In the case of applying fire, the failure is a local failure at the four joints at the source of the temperature.

References

Alinia, M. M., and Kashizadeh. S. (2006), "Effect of flexibility of substructures upon thermal behavior of spherical double layer space truss domes. Part I: uniform thermal loading", *J. Constr. Steel Res.*, **62**, 359–368.

Alinia, M. M., and Kashizadeh. S. (2006), "Effect of flexibility of substructures upon thermal behavior of spherical double layer space truss domes. Part II: gradient & partial loading", *J. Constr. Steel Res.*, **62**, 675–681.

Bakr, H., "Nonlinear Behavior of Composite Space Trusses under Earthquake Loads,"Ms.c. Dissertation, Minoufia University, Egypt, 2014.

Bakr, H., Eltaly, B., El-abd, M., and Kandil, K., "Finite Element Simulation of Space Trusses under Seismic Loads," Malaysian Journal of Civil Engineering, Vol. 28, No. 1, pp. 69- 90, 2016.

Bujakas V. I. (1998), "Shape Control and Kinematic Waves in Large Statically Determinate Structures in Space", *Int. J. Space Struct.*, **1**(13).

Chilton J. (2000) "*Space Grid Structures*", Great Britain: Architectural Press.

Collins, I. M. (1981), "Collapse analysis of double-layer grids", Ph.D. Thesis, Surrey University, Guildford, England.

De Andrade, S. A., da S. Vellasco, P. C., da Silva, J. G., de Lima, J. G., and D'Este, A. V. (2005), "Tubular space trusses with simple and reinforced end-flattened nodes-an overview and experiments", *J. Constr. Steel Res.*, **61**, 1025–1050.

El- Sheikh, A.I. and El-Bakry, H. F. (1996) "Experimental study of behavior of new space truss system", J. of Struct. Eng., ASCE, **122**(8), 845-853.

El-Bakry, H. F. (1995), "Development of A new space truss system", Ph.D. Dissertation, University of Dundee.

El-Shami, M., Mahmoud, S. and Elabd M., (2016), "Effect of floor openings on the capacity of composite space trusses," *J., King Saud University – Eng. Sciences*, Accepted 16 March 2016.

El-Sheikh, A. I. (1991), "The effect of composite action on the behavior of space structures", Ph.D. thesis, University of Cambridge, Department of Engineering, England.

EL-Sheikh, A. I. (1996), "Development of a new space truss system", *J. Constr. Steel Res.,* **37**(3), 205-227.

Eltaly, B. (2010), "Nonlinear behavior of composite space truss", Ph.D. Dissertation, Menoufia University, Egypt.

Feng, F., Menghan S., and Xudong, Z., (2016) "Simplified design method and seismic performance of space trusses with consideration of the influence of the stiffness of their lower supporting columns," Earthq Eng & Eng Vib, **15 (2)**, 401-40.

Hanaor, A., Marsh, C. and Parke, G. A. (1989), "Modification of behavior of double – layer grids: overview", *J. Struct. Div.*, ASCE, **115**(5), 1021 – 1037.

Iffland, J. (1982), "Preliminary planning of steel roof space trusses", *J. Struct. Div.*, ASCE, **108**(ST11), 2578-2591.

Iffland, J. (1987), "*Preliminary Design of Space Trusses and Frames*", Building Structural Design Handbook, Wiley-Interscience Publication, New York.

Lan, T. T. (1985), "Space structures in china", *Int. J. Space Struct.*, 1(5), 155-160, London, England.

Lan, T. T. (1999), "*Space Frame Structures*", Structural Engineering Handbook, Chen Wai-Fah, Boca Raton: CRC Press LLC, Beijing, China.

Mezzina, M., Prete, G., and Tosto, A. (1975), "Automatic and experimental analysis for a model of space grid in elasto-plastic behavior", *Proceedings of Second International Conference on Space Structures*, Surrey, England.

Nawer, M. (2014), "Nonlinear behavior of space trusses with sandwich panels", MS.C. Thesis, Menoufia University, Egypt.

Schmidt, L. C., and Hanaor, A. (1979), "Force limiting devices in space trusses", *J. Struct. Div.*, ASCE, **150**(ST5), 939-951.

Schmidt, L. C., Morgan, P, R., and Clarkson, J. A. (1976), "Space trusses with brittle-type strut buckling", *J. Struct. Div.*, ASCE, **112**(ST7), 1479-1492.

Schmidt, L.C., Morgan, P.R., and Hanaor, A. (1982), "Ultimate load testing of space trusses", *J. Struct. Div.*, ASCE, **108**(ST6), 1324 – 1335.

Shaaban, H. F. (1997), "Effect of composite action on a space truss system with continuous chord members," Ph. D. Dissertation, University of Dundee, UK.

Smith, E. M., (1988), "Alternate path analysis of space trusses for progressive collapse", J. *Struct. Div.*, ASCE, **114**(9), 1978 – 1999.

Yarza, A., Pavia, P., and Parke, G. (1993), "An introduction to the fire analysis of double-layer grids", *Space struct. 4*, G. A. R. Parke and C. M. Howard, eds., Thomas Telford, **1**(5), 683-691.